http://dx.doi.org/10.35596/1729-7648-2025-23-2-28-34

UDC 621.794.61

FIRST-PRINCIPLES MODELING OF ELECTRON-PHONON SCATTERING RATES IN HYDROGENATED GRAPHENE

V. N. MISHCHANKA

Belarusian State University of Informatics and Radioelectronics (Minsk, Republic of Belarus)

Abstract. Graphene, a representative of a new generation of 2D materials, remains in the center of scientific research as a reflection of its unique electrical and mechanical properties. The article presents the results of a study of electron scattering procedures of optical and acoustic phonons in graphene modified with hydrogen atoms, a C_2H_2 structure known as graphane. The obtained dependences of the scattering rates take into account the combined processes of phonon emission and absorption by electrons, but the interaction of phonons with the substrate material is not considered. The scattering rates play an important role in a detailed study of the dynamics of charge carrier transport in semiconductor structures containing heterogeneous layers. Their use makes it possible to implement the well-known many-particle Monte Carlo method, widely used in modeling complex semiconductor devices. The obtained results will allow us to study new heterostructured devices based on graphene and its modifications with improved output characteristics in high-frequency operating ranges.

Keywords: graphene, phonon, modelling, semiconductor structure.

For citation. Mishchanka V. N. (2025) First-Principles Modeling of Electron-Phonon Scattering Rates in Hydrogenated Graphene. *Doklady BGUIR*. 23 (2), 28–34. http://dx.doi.org/10.35596/1729-7648-2025-23-2-28-34.

МОДЕЛИРОВАНИЕ ИЗ ПЕРВЫХ ПРИНЦИПОВ ИНТЕНСИВНОСТЕЙ ЭЛЕКТРОННО-ФОНОННОГО РАССЕИВАНИЯ В ГИДРИРОВАННОМ ГРАФЕНЕ

В. Н. МИЩЕНКО

Белорусский государственный университет информатики и радиоэлектроники (Минск, Республика Беларусь)

Аннотация. Графен, представитель нового поколения 2D-материалов, остается в центре внимания научных исследований как отражение его уникальных электрических и механических характеристик. В статье излагаются результаты исследования процедур электронного рассеяния оптических и акустических фононов в графене, модифицированном атомами водорода, – структуре C_2H_2, известной как графан. В полученных зависимостях скоростей рассеяния учтены совместные процессы испускания и поглощения фононов электронами, а взаимодействие фононов с материалом подложки не рассматривалось. Интенсивности рассеяния играют важную роль для детального изучения динамики транспорта носителей заряда в полупроводниковых структурах, содержащих гетерогенные слои. Их использование позволяет реализовать известный многочастичный метод Монте-Карло, широко применяемый при моделировании сложных полупроводниковых приборов. Полученные результаты позволят исследовать новые гетероструктурные приборы на основе графена и его модификаций с улучшенными выходными характеристиками в высокочастотных диапазонах работы.

Ключевые слова: графен, фонон, моделирование, полупроводниковая структура.

Для цитирования. Мищенко, В. Н. Моделирование из первых принципов интенсивностей электронно-фононного рассеивания в гидрированном графене / В. Н. Мищенко // Доклады БГУИР. 2025. Т. 23, № 2. С. 28–34. http://dx.doi.org/10.35596/1729-7648-2025-23-2-28-34.

Introduction

The study of new two-dimensional materials, among which we should particularly mention graphene and its modifications [1, 2], attracts increased attention of researchers. The charge carrier transport characteristics is constantly in the center attention, due to the fact that such phenomena determine the output performance characteristics of semiconductor devices. In the initial stages of the research, the predominant approach was to develop empirical analytical expressions for scattering rates associated with their various mechanisms, including scattering on optical and acoustic phonons [3–7]. However, the use of a number of simplifying assumptions, and in particular, the assumption of parabolic nature of the energy dependence on the magnitude of the wave vector, without taking into account anisotropy, as well as the need for empirical selection of a number of parameters limits the wide application of this direction in modelling.

New, progressive possibilities for the study of electron transport processes have opened up using a fully *ab initio* approach, which is based on the DFPT (density functional perturbation theory) and the application of Wannier functions to interpolate the obtained results. This approach allows to obtain more accurate values of phonon scattering rates in comparison with experimental measurements of electron and hole mobility and conductivity [8, 9].

In this work, first-principles modeling of electron-phonon scattering rates in hydrogenated graphene has been presented. The use of the obtained modelling results will make it possible to investigate in detail the contribution of various phonon scattering mechanisms in charge carrier transport processes for the complex semiconductor structures.

Method of modeling of electron-phonon scattering rates in hydrogenated graphene

Quantum Espresso [10] and EPW [11, 12] programs were used for the first-principles simulations of hydrogenated graphene (graphane) C_2H_2 type. Perdew-Burke-Ernzerhof (PBE) parametrization within the local density approximation (LDA) and norm-conserving type of the pseudopotentials [13] were used. Next parameters were applied [14]: the cutoff energy of the wave function was 60 Ry (1 Ry ≈ 13.605 eV), the cutoff energy of the charge density and potentials was 240 Ry. The Brillouin zone (BZ) was represented using a 12×12×1 Monkhorst-Pack grid. A vacuum layer of 20 Å thickness (1 Å = $1 \cdot 10^{-10}$ m) was added to the considered structure to avoid unphysical situation during the simulation [14].

The EPW program [11, 12] was used to calculated the scattering rates. At first, the imaginary part of the eigen energy was calculated by

$$\mathrm{Im}\left(\sum\nolimits_{n,\mathbf{k}}^{e-ph}\right) = \pi \sum_{m\nu} \int \frac{d\mathbf{q}'}{\Omega_{\mathrm{BZ}}} \left| g_{mn\nu}\left(\mathbf{k},\mathbf{q}\right)\right|^2 \times$$

$$\times \left\{ \left(n_{\mathbf{q}\nu} + f_{m\mathbf{k}+\mathbf{q}} \right) \delta\left(\left(\varepsilon_{n\mathbf{k}} - \varepsilon_{m\mathbf{k}+\mathbf{q}} \right) + \omega_{\mathbf{q}\nu}\hbar \right) + \left(1 + n_{\mathbf{q}\nu} - f_{m\mathbf{k}+\mathbf{q}} \right) \delta\left(\left(\varepsilon_{n\mathbf{k}} - \varepsilon_{m\mathbf{k}+\mathbf{q}} \right) - \omega_{\mathbf{q}\nu}\hbar \right) \right\}, \quad (1)$$

where $\hbar$ is the modified Plank constant; $\varepsilon_{n\mathbf{k}}$, $\varepsilon_{m\mathbf{k}+\mathbf{q}}$ are the energies for the bands with number n and wavevector $\mathbf{k}$ and number m and wavevector $\mathbf{k+q}$ in the Bruellen zone (Ω_{BZ}); $\omega_{\mathbf{q}\nu}$ is the phonon frequency with mode ν and wave vector $\mathbf{q}$ in the BZ over which the integration is performed; $f_{m\mathbf{k}+\mathbf{q}}$, $n_{\mathbf{q}\nu}$ are the Fermi and Bose distributions, respectively, which are estimated at a given temperature; $g_{mn\nu}(\mathbf{k}, \mathbf{q})$ is the electron-phonon interaction matrix; δ is the necessity of performing Gaussian smoothing operations during integration [14].

The scattering rates with phonon absorption and emission were calculated from formula [12, 15]

$$\tau^{-1} = 2/\hbar \cdot \mathrm{Im}\left(\sum\nolimits_{n,\mathbf{k}}^{e-ph}\right). \quad (2)$$

The following values of the modeling parameters were selected in the EPW program [14]: the size of grid $N \times N \times 1$ was 264×264×1; Gaussian smoothing coefficient (parameter "dg") – equal to 0.001 eV; the parameter "fsthick", which determines the value of the range of energies during modeling relative to the Fermi energy level, – equal to 4 eV; the number of Wannier functions – equal to 12. Parameters "auto_projection" and "scdm_proj" were set to "true". Concentration of electrons and holes for all calculations is set to $1 \cdot 10^{13}$ cm^{-3} [14].

Results from first principles calculation of the scattering rates in hydrogenated graphene

It is known that ZA, TA, LA, LB, TB, LB*, TB*, ZO, TO, LO, ZS, ZS* phonon modes are formed in hydrogenated graphene of the C_2H_2 type [16]. Modes, denoted as LA, TA, ZA, are results of the scattering on acoustic phonons along the longitudinal and transverse directions (x, y coordinates), and the z coordinate orthogonal to them [16]. Modes, denoted as LO, TO, ZO, are results of scattering on optical phonons along the longitudinal and transverse directions (x, y coordinates), and the z coordinate orthogonal to them [16].

Hydrogenated graphene C_2H_2 type (graphane) in comparison with graphene have the processes of structure bending, which are presented by the two symmetric modes - longitudinal and transverse LB and TB, and two asymmetric modes LB* and TB* [16]. In the z direction two modes associated with stretching processes are formed – the symmetric mode ZS and asymmetric mode ZS* [16]. The dependences the scattering rates for modes ZA, TA, LA, LB, TB, LB*, TB*, ZO, TO, LO, ZS, ZS* from energy obtained in the EPW program using formulas (1), (2) are presented in Fig. 1–12 by color dots.

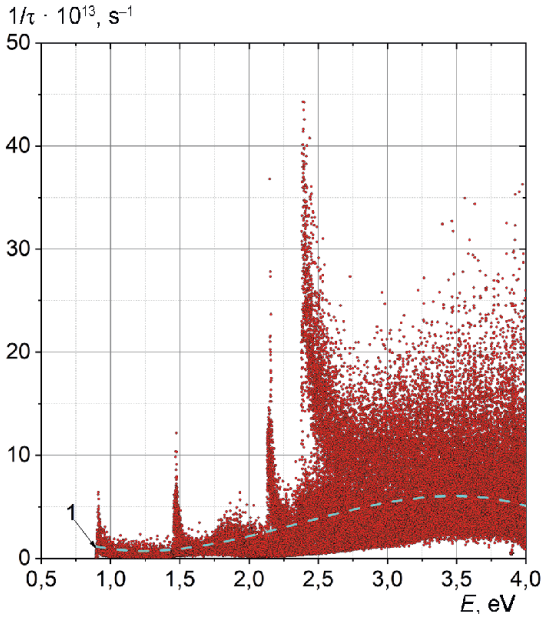

Fig. 1. Scattering rates for the acoustic mode ZA on energy

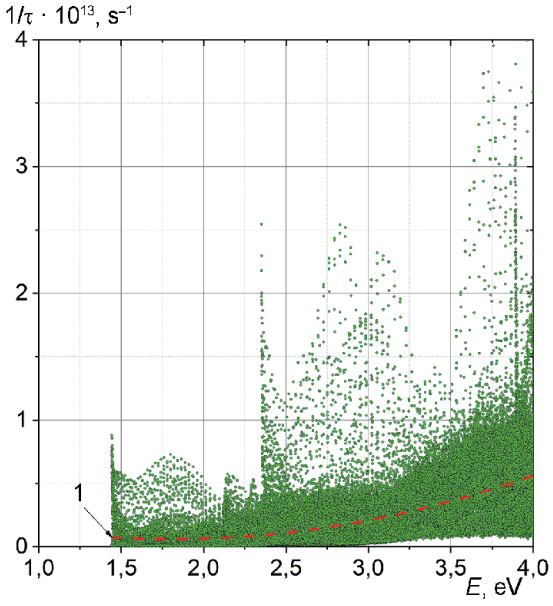

Fig. 2. Scattering rates for the acoustic mode TA on energy

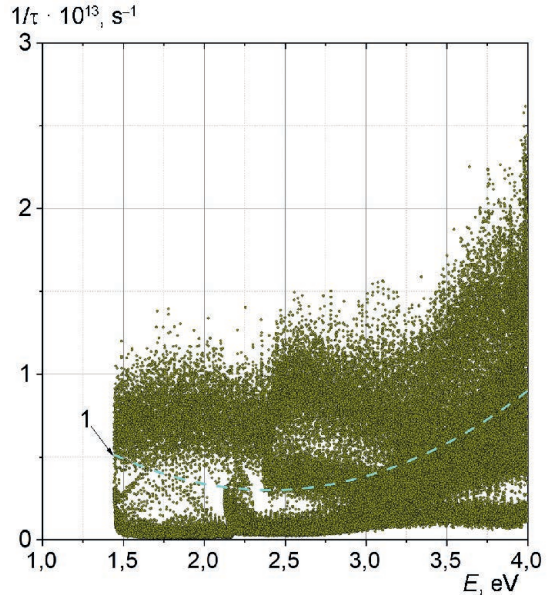

Fig. 3. Scattering rates for the LA acoustic mode on the energy

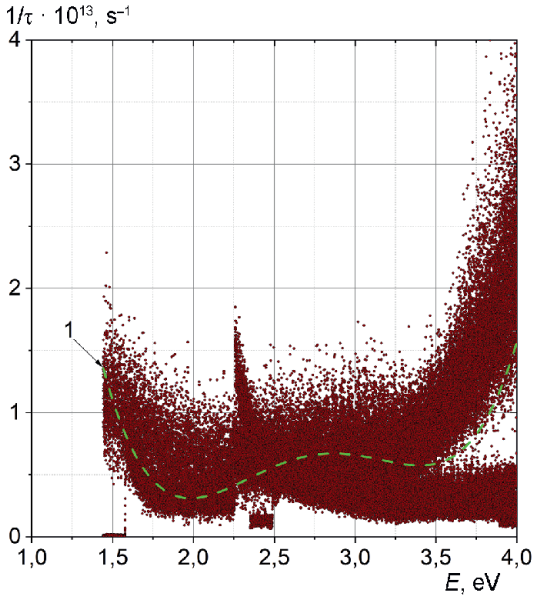

Fig. 4. Scattering rates for the LB mode on the energy

Data processing and plotting program ORIGIN is permitted to complete of approximation of the point data using analytic degree functions the with the help of the Fitting and Polinomial Fit operations in the Analysis section [17]. The Origin program provides the minimum value of the approximation error of the obtained data sets for all scattering intensities inherent to a given material. Approximation of the first-principles modeling data was completed with the help of the ORIGIN program. The results for the modes ZA, TA, LA, LB, TB, LB*, TB*, ZO, TO, LO, ZS, ZS* are shown in Tab. 1. Analytical relationships presented in Tab. 1 were used to plotted the curves 1, which are shown in Fig. 1–12.

Table 1. Results of approximation of first-principles modeling data for the parameter τ^{-1} (s^{-1}) from the energy E (eV)

Type of mode	Type of dependences	Number of the figure where the dependency is represented as a curve 1
ZA	$\tau^{-1} = \left(24 - 39,6215E + 21,6613E^2 - 3,05675E^3\right)\cdot 10^{13}$	1
TA	$\tau^{-1} = \left(1,30817 - 1,22865E + 0,34054E^2\right)\cdot 10^{13}$	2
LA	$\tau^{-1} = \left(5,4136 - 3,68907E + 0,768924E^2\right)\cdot 10^{13}$	3
LB	$\tau^{-1} = \left(40 - 62,335E - 35,75905E^2 - 8,86966E^3 + 0,80633E^4\right)\cdot 10^{13}$	4
TB	$\tau^{-1} = \left(0,02 - 0,1067324E + 0,14873E^2 - 0,06888E^3 + 0,01184E^4\right)\cdot 10^{13}$	5
LB*	$\tau^{-1} = \left(0,25 - 0,67324E + 0,62945E^2 - 0,23297E^3 + 0,03156E^4\right)\cdot 10^{13}$	6
TB*	$\tau^{-1} = \left(0,5 - 1,39387E + 1,33834E^2 - 0,50374E^3 + 0,06808E^4\right)\cdot 10^{13}$	7
ZO	$\tau^{-1} = \left(10^{-4} - 0,64273E + 1,40924E^2 - 0,76814E^3 + 0,13122E^4\right)\cdot 10^{13}$	8
TO	$\tau^{-1} = \left(0,65187E - 0,6714E^2 + 0,16824E^3 + 0,00383E^4\right)\cdot 10^{13}$	9
LO	$\tau^{-1} = \left(1,77365E - 2,15171E^2 + 0,77598E^3 - 0,05832E^4\right)\cdot 10^{13}$	10
ZS	$\tau^{-1} = \left(18,4954E - 15,35071E^2 + 4,50152E^3 - 0,43377E^4\right)\cdot 10^{13}$	11
ZS*	$\tau^{-1} = \left(1,86807E - 1,8118E^2 + 0,47577E^3 - 0,01522E^4\right)\cdot 10^{13}$	12

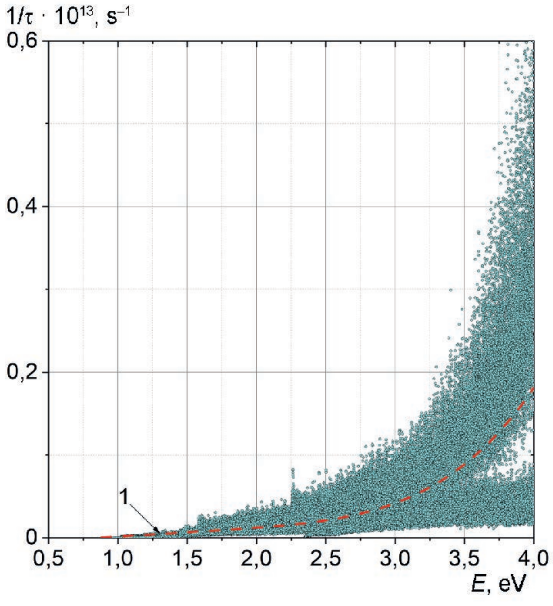

Fig. 5. Scattering rates for the TB mode on the energy

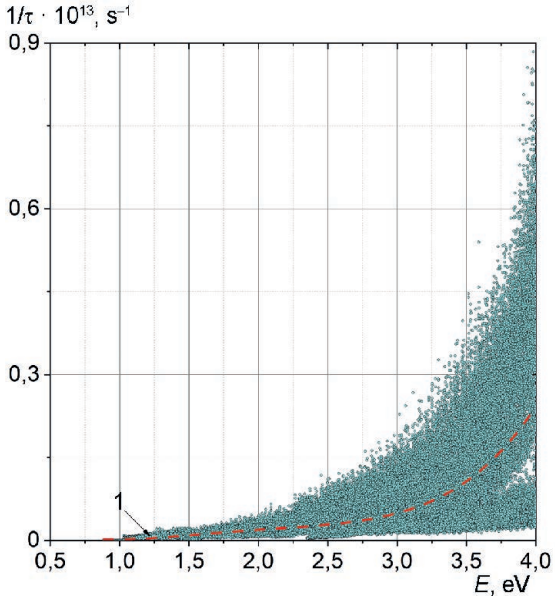

Fig. 6. Scattering rates for the LB* mode on the energy

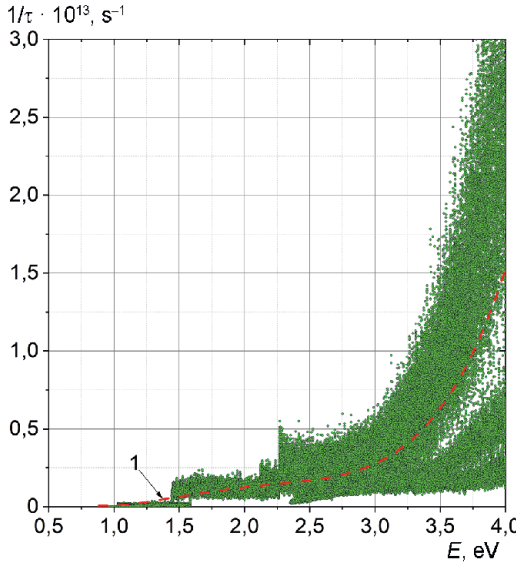

Fig. 7. Scattering rates for TB* optical mode on energy

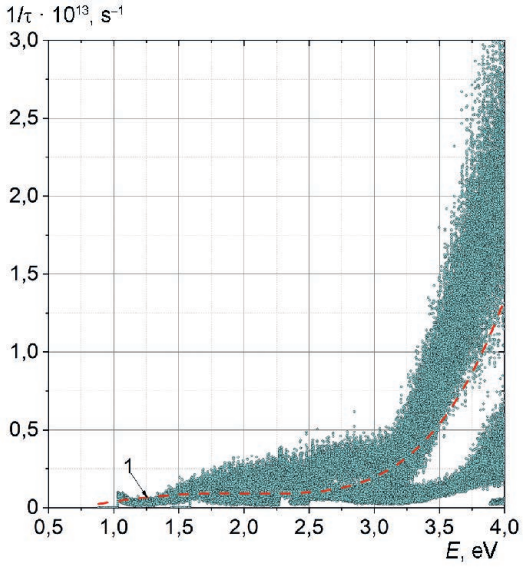

Fig. 8. Scattering rates for ZO optical mode on energy

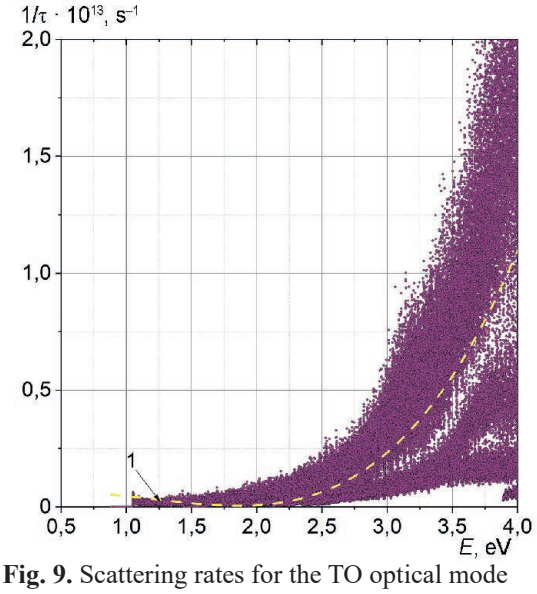

Fig. 9. Scattering rates for the TO optical mode on energy

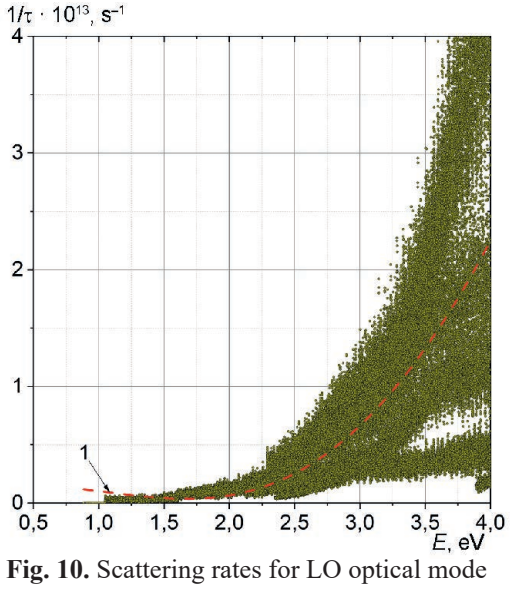

Fig. 10. Scattering rates for LO optical mode on energy

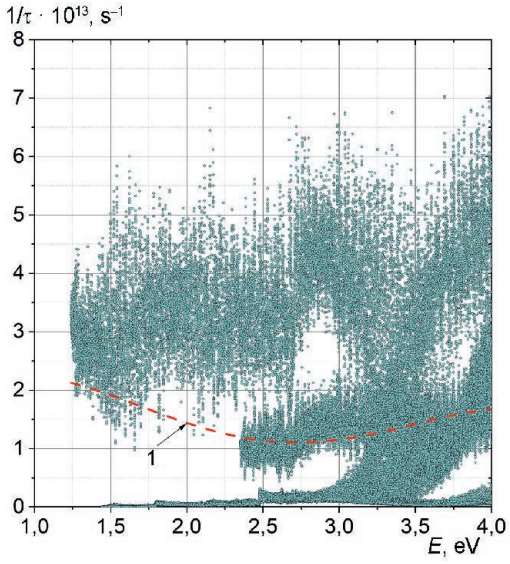

Fig. 11. Scattering rates for the ZS optical mode on energy

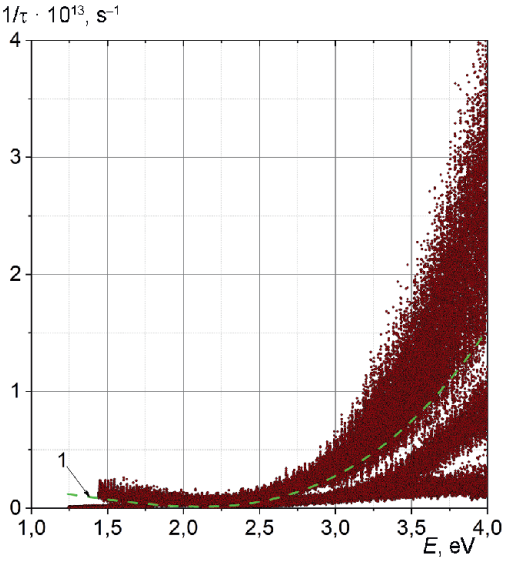

Fig. 12. Scattering rates for the ZS* optical mode on energy

Using data presented in Tab. 1 curves of scattering rates have been calculated for optical modes ZO, TO, LO (Fig. 13, curves 1–3) and for acoustic modes ZA, TA, LA (Fig. 14, curves 1–3).

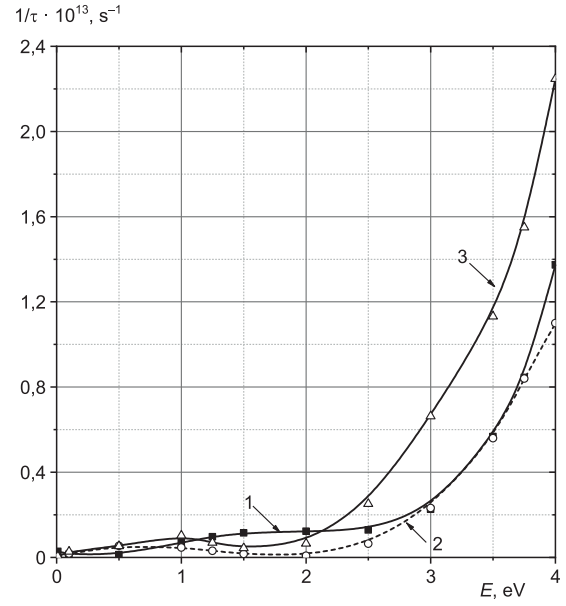

Fig. 13. Scattering rates on energy in the case of ZO (curve 1), TO (2) and LO (3) optical modes

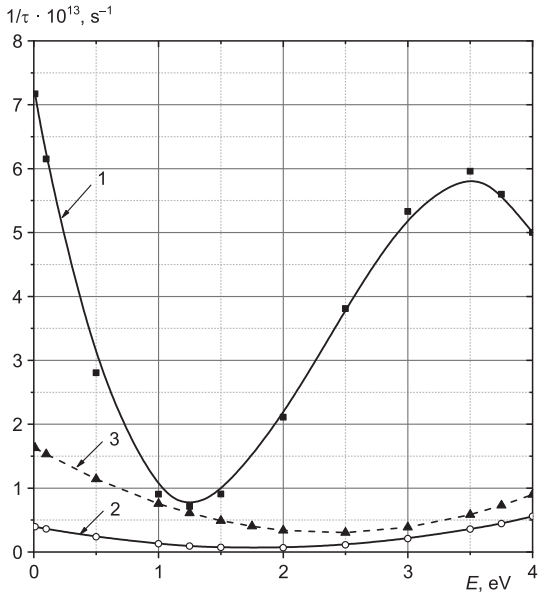

Fig. 14. Scattering rates on energy in the case of ZA (curve 1), TA (2) and LA(3) acoustic modes

Using data presented in Tab. 1 scattering rates have been calculated in the case of ZS and ZS* (Fig. 15, curve 1, 2) and in the case of LB, TB, LB*and TB* mode (Fig. 16, curve 1–4).

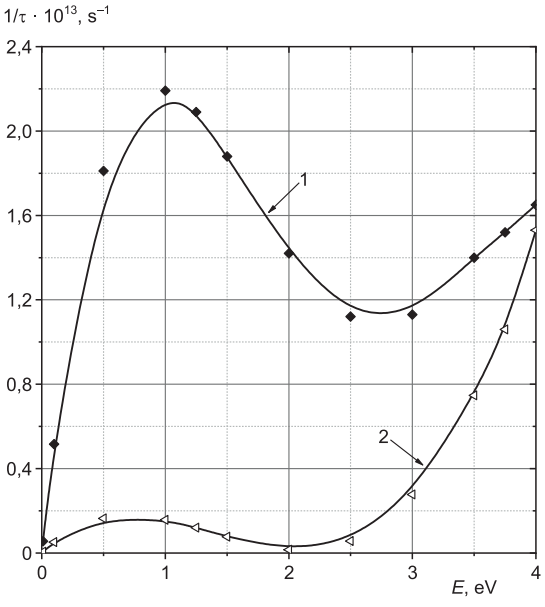

Fig. 15. Scattering rates on energy in the case of ZS (curve 1) and ZS* (2) modes

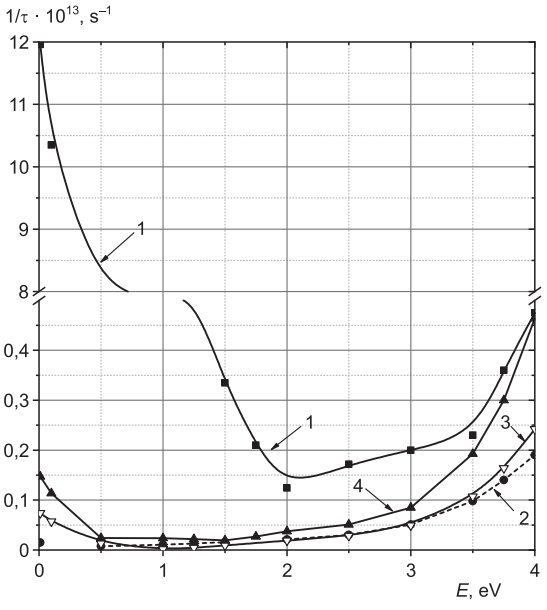

Fig. 16. Scattering rates on energy in the case of LB (curve 1), TB (2), LB* (3), and TB* (4) modes

The largest scattering rates are observed for the LB mode for small energy value less than 1 eV (Fig. 13–16). Modes ZA, ZO, LO, TO, ZS, ZS* have largest scattering rates at the energy greater than 4 eV. Scattering rates of the modes LB, LB*, TB, TB*, TA, LA are smaller than the scattering rates for the modes ZA, ZO, LO, TO, ZS, ZS* for the energy less than 4 eV. The scattering rates of modes LO, TO and ZO are close to each other in energy range which not exceeds 4 eV.

Conclusion

The dependences of electron scattering rates on optical and acoustic phonons in the free layer of hydrogenated graphene of C_2H_2 type (graphane) have been studied. First-principles modelling for modes ZA, TA, LA, ZO, TO, LO, LB, TB, LB*, TB*, ZS, ZS* types has shown that the highest scattering intensity at low energies (less than 1 eV) is observed for the LB-type mode, which is presented a longitudinal symmetric mode associated with the process of structure bending. At significant energy values, which exceed 4 eV, the usual optical modes – longitudinal LO, transverse TO, as well as modes along the z direction – optical ZO and acoustic ZA – already dominate in magnitude. The obtained numerical data on the behaviour of electron scattering rates dependences for graphene modified by hydrogen atoms can be used to study the characteristics of new promising semiconductor devices using the Monte Carlo method.

References

1. Novoselov K. S., Geim A. K., Morozov S. V., Jiang D., Zhang Y., Dubonos S. V., Grigorieva I. V., et al. (2004) Electric Field Effect in Atomically Thin Carbon Film. *Science.* 306, 666–669.
2. Morozov S. V., Novoselov K. S., Katsnelson M. I., Schedin F., Elias D. C., Jaszczak J. A., et al. (2008) Giant Intrinsic Carrier Mobilities in Graphene and Its Bilayer. *Physical Review Letters.* 100.
3. Bardeen J., Shockley W. (1950) Deformation Potentials and Mobilities in Nonpolar Crystals. *Physical Review.* 80. https://doi.org/10.1103/PhysRev.80.72.
4. Herring C., Vogt E. (1956) Transport and Deformation-Potential Theory for Many-Valley Semiconductors with Anisotropic Scattering. *Physical Review.* 101.
5. Fröhlich H. (1954) Electrons in Lattice Fields. *Advances in Physics*. 3.
6. Hess K. (1999) *Advanced Theory of Semiconductor Devices*. NJ, Wiley-IEEE Press, Piscataway.
7. Lundstrom M. (2009) *Fundamentals of Carrier Transport*. UK, Cambridge University Press, Cambridge.
8. Poncé S., Margine E. R., Verdi C., Giustino F. (2016) EPW: Electron-Phonon Coupling, Transport and Superconducting Properties Using Maximally Localized Wannier Functions. *Computer Physics Communications*. 209.
9. Zhou J.-J., Park J., Lu I-Te, Maliyov I., Tong X., Bernardi M. (2021) Perturbo: A Software Package for *ab Initio* Electron-Phonon Interactions, Charge Transport and Ultrafast Dynamics. *Computer Physics Communications*. 264.
10. Giannozzi P., Baroni S., Bonini N., Calandra M., Car R., Cavazzoni C., et al. (2009) QUANTUM ESPRESSO: A Modular and Open-Source Software Project for Quantum Simulations of Materials. *Journal of Physics: Condensed Matter.* 21 (39).
11. Noffsinger Jesse, Giustino Feliciano, Malone Brad D., Cheol-Hwan Park, Louie Steven G., Cohen Marvin L. (2010) EPW: A Program for Calculating the Electron–Phonon Coupling Using Maximally Localized Wannier Functions. *Computer Physics Communications.* 181 (12), 2140–2148.
12. Lee H., Poncé S., Bushick K., Hajinazar S., Lafuente-Bartolome J., Leveillee J., et al. (2023) Electron-Phonon Physics from First Principles Using the EPW Code. *npj Computational Materials*. 9.
13. Hamann D. R. (2013) Optimized Norm-Conserving Vanderbilt Pseudopotentials. *Physical Review.* B 88.
14. Mishchanka V. N. (2024) First-Principles Modeling of Electron-Phonon Scattering Rates in Graphene. *Modern Electronic Materials.* 10 (3), 177–184.
15. Bernardi M., Vigil-Fowler D., Lischner J., Neaton J. B., Louie S. G. (2014) *Ab Initio* Study of Hot Carriers in the First Picosecond after Sunlight Absorption in Silicon. *Physical Review Letters.* 112.
16. Long Cheng, Chenmu Zhang and Yuanyue Liu (2019) How to Resolve a Phonon-Associated Property into Contributions of Basic Phonon Modes. *Journal of Physics: Materials*. 2 (4).
17. Isakova O. P., Tarasevich Y. Y., Yuzyuk Y. I. (2009) *Processing and Visualization of Data from Physical Experiments Using Origin Package*. Moscow, LIB-COM Book House.

Received: 19 January 2025 Accepted: 28 February 2025

Information about the author

Mishchanka V. N., Cand. Sci. (Tech.), Associate Professor, Belarusian State University of Informatics and Radioelectronics

Address for correspondence

220013, Republic of Belarus, Minsk, P. Brovki St., 6
Belarusian State University of Informatics and Radioelectronics
Tel.: 375 29 394-55-58
E-mail: mishchenko@bsuir.by
Mishchanka Valery Nikolaevich